Biointerface Research in Applied Chemistry
Open-Access Journal (ISSN: 2069-5837)

Article
Volume 13, Issue 1, 2023, 11
https://doi.org/10.33263/BRIAC131.011

Immobilization of Glucose Oxidase on pH-Responsive Polyimide-Polyacrylic Acid Smart Membranes Fabricated Using 248 nm KrF Excimer Laser for Drug Delivery

Renuka Subhash Patil [1], Amal Narayanan [1], Chinnapatch Tantisuwanno [1], Erol Sancaktar [1,*]

[1] School of Polymer Science and Polymer Engineering, University of Akron, OH 44325, USA; rsp44@uakron.edu (R.P.), an75@uakron.edu (A.N.), ct75@uakron.edu (C.T.), erol@uakron.edu (E.S.);
* Correspondence: erol@uakron.edu (E.S.);

Scopus Author ID **7004834161**
Received: 4.09.2021; Accepted: 15.11.2021; Published: 18.01.2022

Abstract: The permeability of polyimide–polyacrylic acid (PI-PAAc) pH-responsive membrane fabricated using a 248 nm KrF laser was investigated. These membranes were further immobilized with glucose oxidase enzyme, which led to the successful development of a glucose-responsive membrane. The base PI membranes were developed using a simple photolithographic technique. Further grafting of PAAc inside the pores was carried out using the same laser wavelength. The effect of various solution parameters and laser parameters were studied and discussed in detail in our previous work. A variety of grafting yields were obtained by changing laser exposure time. Glucose Oxidase (GOD) enzyme was then immobilized on the membrane using a carbodiimide-based amidation method. The polyacrylic acid grafted inside the pores shows pH-responsive gating. The immobilized GOD molecules show glucose sensitivity and convert the glucose into gluconic acid. The experiment results show that these membranes can detect the amount of glucose and release the corresponding solute amount.

Keywords: Excimer laser; immobilization; responsive membranes; grafting.

1. Introduction

Stimuli-responsive membranes are designed for a specific application and thus are of foremost importance [1–9]. Especially, pH-responsive membranes have applications in separation processes, sensor applications, and controlled drug release applications [10,11]. The human gastrointestinal tract has a considerable variation in pH value [12–14]. Therefore, the pH-responsive membranes can be very useful for controlled drug release in the human body to target specific areas or organs [15,16]. Although there are pH-responsive 3D crosslinked structures available for controlled drug release, gating membranes offer the advantage of their immediate response compared to their hydrogel analogs [17]. In the case of controlled drug release systems, it is essential to release drugs as soon as the system receives the environmental stimulus [15,18,19]. Herein, a reservoir-based controlled release drug system for diabetes is studied.

Diabetes is a major health issue in industrialized countries [20]. Especially during current CIVID times [21–23]. Although many medications are available on the market, they have adverse effects like gastric irradiation, nausea, and many more [24]. The very common treatment for a diabetic patient is insulin injection into the body [25]. However, the poor control of glucose level in blood after the injection is a major concern in maintaining homeostasis [17].

Besides, the amount of glucose level is different during different meals like breakfast, lunch, dinner, and the rest of the day [26]. It also depends on the type of food one eats. Therefore, it is important to have temporal control on insulin release depending on the glucose level in the blood. For this purpose, researchers have proposed that the fabrication of immobilized glucose oxidase (GOD) on pH-responsive membranes may improve the therapeutic efficiency in diabetic patients. For example, GOD enzymatically converts glucose into gluconic acid. The gluconic acid changes the pH of the environment in its vicinity, which helps the pH-responsive membrane release drugs corresponding to the amount of glucose [17,26,27].

We have already developed an ultrafast, solvent-free method to develop a pH-responsive membrane [28,29]. This study further immobilized these membranes with GOD, making them glucose-responsive. The membranes are fabricated using an excimer laser, which reduces the fabrication time significantly [30–32]. Water was used as the solvent in the reaction system, making the grafting system environmentally friendly, providing a significant advantage. Solvents will only be used for cleaning purposes. Polyimide (PI) is a suitable material for membrane fabrication because of its excellent chemical and thermal resistance. PAAc is selected, on the other hand, because of its biocompatibility [33]. In this paper, we aim to use this fabrication technique to develop glucose-responsive membranes that will have potential applications in diabetes treatment.

2. Materials and Methods

Kapton HN PI films - 25 μm thick were obtained from DuPont High-Performance Material (Durham, NC, USA). 20 μm stainless steel mesh (625 mesh) was purchased from TWP Inc (Berkeley, CA, USA). Acrylic acid (AAc), N, N'-methylene bisacrylamide (mBAAm), Irgacure 2959, β-(N-Morpholino) ethane sulfonic acid (MES), D-(+)-Glucose, glucose oxidase aspergillus HI-PU 100KU (GOD), Hydroquinone, Caffeine, acetone, and tetrahydrofuran (THF) were purchased from Sigma Aldrich (St. Louis, MO, USA). Ethanol was purchased from Decon Labs, Inc (King of Prussia, PA, USA). N-(3-dimethyl aminopropyl)-N'-ethyl carbodiimide hydrochloride (EDC) was purchased from Oakwood Chemicals. Rhodamine B and N-hydroxysuccinimide were purchased from VWR. The primary amine-terminated Rhodamine (Rhodamine-NH_2) was synthesized in the lab using previously reported methods [34]. Distilled water, prepared in our lab, was used to prepare grafting solutions. Deionized water with total dissolved solids contents below 5 ppm was used for all other purposes. A 248 nm KrF excimer laser (Lambda Physik 240i) with a pulse width of 25 ns was used for ablative degradation and photo-polymerization.

2.1. Fabrication of base PI membrane.

PI base membrane with an average pore size of 11.24 $\pm$ 1.14 μm was prepared using the lithographic technique in a circular region of 4 mm in the center using fluence 250 mJ/cm^2 and 400 pulses at 1 Hz frequency. Our previous work discussed the fabrication process in detail [28]. Membranes were further cleaned using ethanol and THF for 5 minutes each in a sonicator. They were then dried for 24 hours in a vacuum for the next step, i.e., grafting.

2.2. Grafting polyacrylic acid gates by laser grafting pore-filling polymerization.

For the grafting step, the reaction solution was prepared using AAc monomer (5% w/w), mBAAm (3.5% w/w of monomer) crosslinker, and Irgacure 2959 initiator (1% w/w of monomer). PI membrane was placed on the top of the O-ring, and 90 µL reaction solution was placed on the top of the membrane to be grafted. The solution passes through the pores inside the reservoir (cavity in O-ring below membrane), wetting the membrane walls. The reaction was carried out in the nitrogen environment at a fluence of 5 mJ/cm^2 using various pulse numbers. A laser wavelength of 248 nm was used for both the steps, i.e., base membrane fabrication and grafting. The frequency used for the grafting step is 25 Hz. 5 mg/mL hydroquinone inhibitor solution was used at the end to quench the reaction. Membranes were then washed using DI water to remove the unreacted monomer. Various pulses were used to obtain membranes at different grafting conditions using pulses 400, 800, and 1200.

2.3. Morphological analysis of membrane.

Fourier transform infrared (FT-IR) spectra of the PAAc, ungrafted, and the PAAc-grafted membranes were measured on a spectrophotometer (Alpha-P FTIR Spectrometer, Bruker Optics, MA, USA) after drying membranes at 45 ^{0}C for 24 hours.

To observe the microscopic configuration of PAAc-grafted membranes with different grafting yields, a scanning electron microscope (SEM, JOEL JSM-7401F) was used. Additionally, Fluorescence microscope images were taken using a Laser Scanning Confocal Microscope – (Zeiss LSM-510 fluorescence microscope). Membranes were exposed to the light of wavelength 543 nm, and a 560 nm filter was used to observe the fluorescence.

Thermogravimetric Analysis (TGA) (Q500, TA Instruments) was used to determine the weight of PAAc acid grafted inside the membrane pores. Membranes were dried at 45 ^{0}C for 24 hours before doing TGA.

2.4. Estimation of change in permeability using filtration experiment.

The pH-responsive changes in pore size of the membrane with different grafting yields were determined using a dead-end filtration cell (Amicon 8010, Millipore). A pressure of 0.034 MPa (5 psi) was used to conduct the filtration experiment. Water was allowed to pass across the membrane, and the flux was measured by collecting the water in a container attached to the weighing balance. The weighing balance was connected to the computer, which automatically calculated the water flow rate. Permeability coefficient (permeability) (J) was calculated using equation (1)

$$J = \frac{m}{\rho.\ A.\ \Delta P}\ ,\ (1)$$

where m = water flow rate; ρ = density of water (1 mg/mL); A = area of perforated region; ΔP = applied pressure.

Initially, a membrane grafted using 600 pulses was used. Permeability value changes drastically from pH 3 to pH 7; thus, permeabilities at these two pH levels were calculated for all the membranes.

2.5. Preparation of glucose-responsive membranes using immobilization reaction.

After permeation studies, membrane grafted at 800 pulses was used for the next step, i.e., immobilization of GOD. The immobilization was carried out using the carbodiimide-

catalyzed method [17,35]. First, the PAAc-grafted membrane was placed in an MES buffer at pH 4.75 containing (10 wt%) N-(3-dimethyl aminopropyl)-N'-ethyl carbodiimide hydrochloride (EDC)). EDC was used to activate the carboxylic group present in PAAc. After allowing this reaction for an hour, unreacted EDC was removed after carefully washing the membranes using water at pH 4.75.

EDC coupled samples were further reacted with glucose oxidase (1 wt. %) aqueous solution at pH 4.75 for 24 hours at 4 ^{0}C. The amide bond forms between the amino group present in the glucose oxidase and the carboxylic group in the grafted polyacrylic acid. Membranes were then washed using acidic water in slow stirring for 24 hours and used for diffusion studies.

To confirm that the immobilization reaction occurs, membranes were reacted with Rhodamine- NH_2. After the EDC coupling reaction, the same procedure used for grafting GOD was used for fabricating Rhodamine-conjugated membranes. These membranes were then studied under the fluorescence microscope to confirm the reactivity of PAAc-grafted membranes.

2.6. Diffusion experiments.

After immobilization of GOD, 5 mg/mL caffeine was used as a model drug to carry out-diffusion experiments. The donor vial of 2 mL and the receptor vial of 5 mL was used for the experiment. The donor vial was inverted on the receptor vial using double-sided tape. The membrane was fixed inside the donor vial, and the receptor vial was continuously stirred using a magnetic stirrer. 500 µL aliquots were taken out periodically, and caffeine concentration was found using UV vis spectroscopy. The diffusion coefficient was calculated using Fick's first law of diffusion-

$$ln\left(\frac{C_0-C_f}{C-C_f}\right) = D \cdot \frac{V_d+V_r}{V_d V_r} \cdot \frac{A}{\Delta x} \cdot t \ , \quad (2)$$

where C_0, C and C_f are initial, intermediate (at time t), and final caffeine concentrations, respectively, in donor solution. D is the membrane diffusion coefficient. V_d, V_r are volume of donor and receptor vials, respectively. A is an effective permeation area, and Δx is membrane thickness.

After carrying out immobilization reaction as described previously, diffusion across the membrane was studied in the absence and presence of glucose using various glucose concentrations.

3. Results and Discussion

3.1. Morphological analysis of PAAc grafted membranes.

Figure 1 shows SEM images of PAAc grafted at various grafting yields, i.e., at various numbers of pulses or various exposure times. It can be seen very clearly that each incoming pulse grafting continues by a bottom-up approach. After permeation experiments, these images proved that the grafted material was chemically attached firmly inside the pores. For membrane grafted at 400 pulses, the material appears to have washed away.

To prove that the material grafted inside the pore is PAAc, ATR-FTIR was carried out. Figure 2 shows ATR-FTIR spectra for membranes grafted using PAAc crosslinked network. N-H and O-H groups present in the crosslinked PAAc give broad peaks around 2400 cm^{-1} to 3600 cm^{-1} [36].

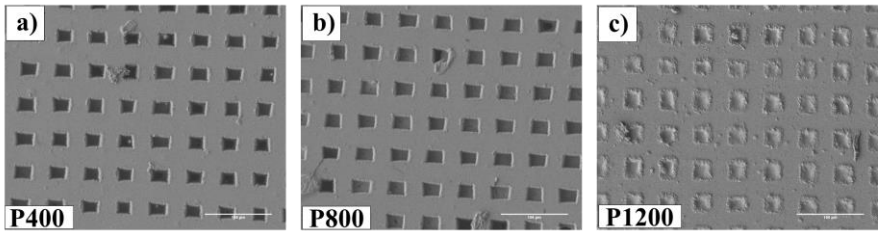

Figure 1. SEM images of grafted membranes manufactured using F250P400Hz1 (11 µm pore size) support membranes. All were prepared using F =5 mJ/cm^2. (a), (b) and (c) were grafted at P400, P800, and P1200, respectively. Scale bar = 100 µm.

N-H stretching peaks were seen at 3485 cm^{-1}, and broad O-H stretching height was around 3042 cm^{-1}. No specific peaks were observed for membrane grafted at 400 pulses at 3485 cm^{-1} and 3042 cm^{-1} since most of the polymer is washed away during permeation studies.

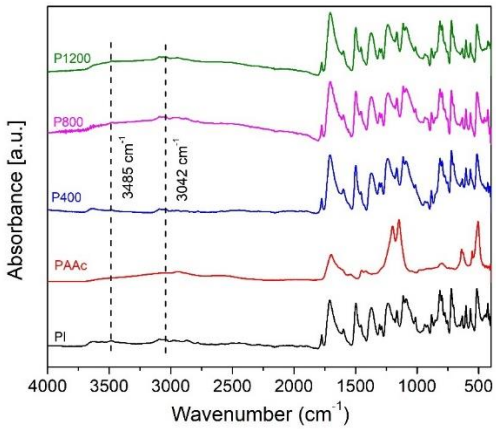

Figure 2. ATR-FTIR spectra of PAAc, PI, and membranes grafted at various pulses.

Fluorescence microscope images figure 3 were taken using Laser Scanning Confocal Microscope - Zeiss LSM-510 fluorescence microscope. After the immobilization reaction, fluorescence can be seen confirming the conjugation reaction of PAAc with the amine-containing molecule.

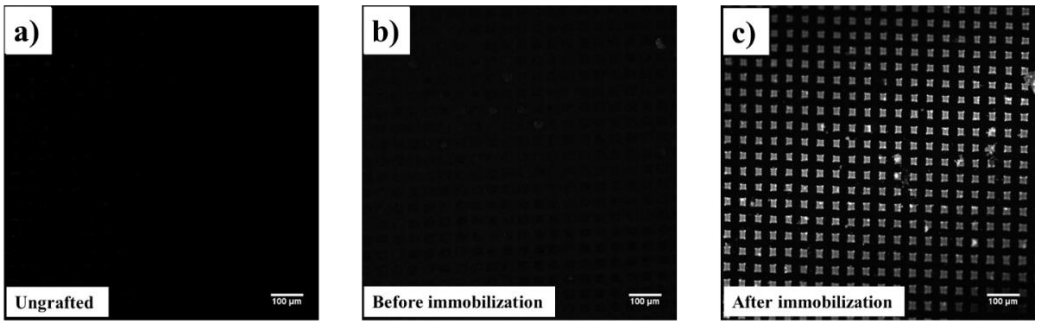

Figure 3. Fluorescent images of grafted membranes exposed to 540 nm wavelength on pore-filled F250P400Hz1 (11 µm pore size) support membranes. (b) and (c) were prepared at F =5 mJ/cm^2. (a) ungrafted, (b) membrane grafted using P800 before carrying out immobilization reaction, (c) membrane grafted using P800 after immobilization reaction with Rhodamine B. All images were taken using lase wavelength of 543 nm and filter 560 nm. Scale bar: 100 µm.

3.2. Effect of PAAc grafting yield on the responsiveness of membrane.

Membranes permeability values show major change at pH 3 and pH 7, as shown by our previous studies [28,29]. Therefore, these two pH levels were chosen for further studies. At higher pH, the polymer swells because of the repulsion between adjacent COO^- groups present

in the polymer chain. On the other hand, it dwells inside the pores at lower pH. Deswelling increases overall pore size, resulting in a higher permeability value than that at lower pH. More material is grafted inside the pore with each incoming laser pulse, restricting the water flow across the membrane, leading to a decrease in the permeability value, as seen in figure 4.

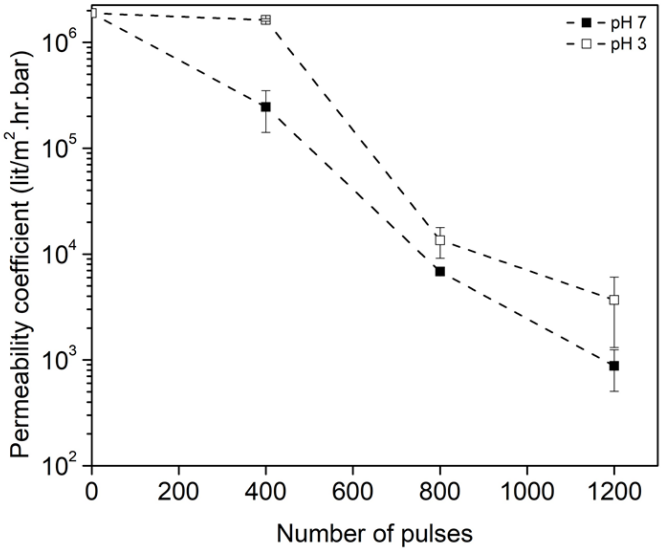

Figure 4. Water permeability of grafted membranes prepared at various pulses.

3.3. Weight of PAAc grafted inside pores.

Since the amount of material grafted inside the pore is just a few mg, TGA was used for determining the weight of material grafted inside the pores. PAAc degrades completely around 500 ºC; on the other hand, PI starts to degrade at 600 ºC, TGA becomes a beneficial and easy tool to determine the weight grafted inside the pores, as seen in figure 5. With an increasing number of pulses, grafted weight increases.

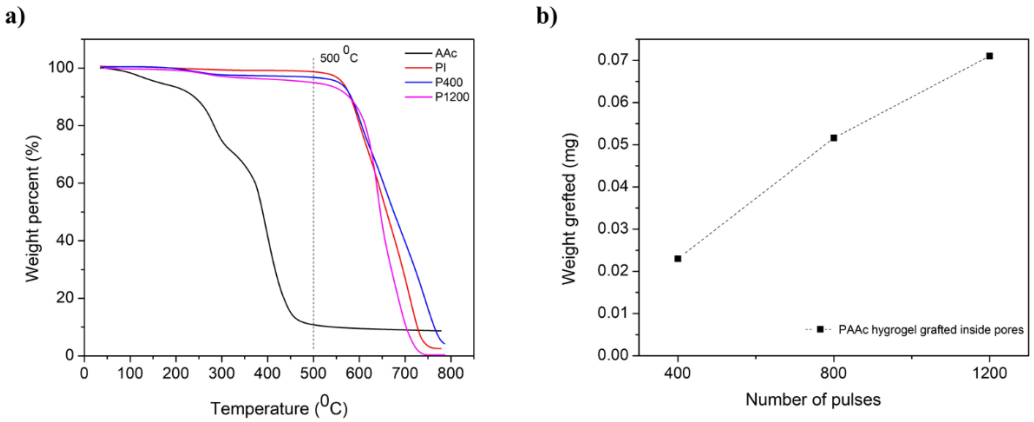

Figure 5. a) TGA curve for crosslinked PAAc hydrogel, PI, and membranes grafted at P400 and P1200; b) Weight of hydrogel grafted as a function of the number of pulses.

3.4. Diffusion permeability.

Figure 6 (a) shows caffeine permeation across the membrane before and after glucose addition. After adding glucose, solute permeation increases, and this increase is almost linear. Diffusion coefficient increases with increasing the amount of glucose. This implies that the

membranes can detect the amount of glucose and release the corresponding amount of solute molecule.

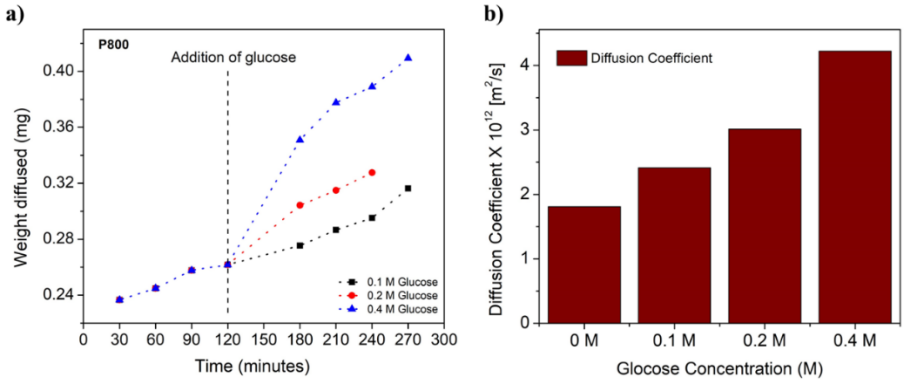

Figure 6. (a) Caffeine diffusion through the membrane grafted at P800 after immobilization reaction; (b) Diffusion coefficient of caffeine calculated after diffusion studies.

4. Conclusions

The membrane fabrication technique used in this paper is entirely organic solvent-free, and fast. Using laser lithographic techniques, pores obtained on the base membrane led to uniform, regular, and ordered pores. The grafting step uses the same laser wavelength to fill the pores with pH-responsive polymer hydrogel. The process does not involve any organic solvents. The membrane fabrication time is significantly low. It takes only twenty seconds to obtain the grafted membrane.

Further immobilization of this membrane results in glucose-responsive smart membranes. The membrane gives an almost linear drug release profile, and the amount of drug released also corresponds to the glucose level. This membrane shows a potential application for diabetes treatment because of its ability to detect glucose levels and release the corresponding solute.

Funding

This research received no external funding.

Acknowledgments

The authors greatly acknowledge the continuous support of Dr. Erol Sancaktar and the School of Polymer Science and Polymer Engineering, University of Akron, for financial support. The author would also like to thank Dr. A. Joy for allowing their facilities. Special thanks are also due to Dr. Ankit Tiwari and Mr. Leyao Wu for guidance and time.

Conflicts of Interest

The authors declare no conflict of interest.

References

1. Zhang, Z.; Xiao, X.; Zhou, Y.; Huang, L.; Wang, Y.; Rong, Q.; Han, Z.; Qu, H.; Zhu, Z.; Xu, S.; Tang, J.; Chen, J. Bioinspired Graphene Oxide Membranes with PH-Responsive Nanochannels for High-Performance Nanofiltration. *ACS Nano* **2021**, *15*, 13178–13187, https://doi.org/10.1021/acsnano.1c02719.

2. Li, L.; Rong, L.; Xu, Z.; Wang, B.; Feng, X.; Mao, Z.; Xu, H.; Yuan, J.; Liu, S.; Sui, X. Cellulosic Sponges with PH Responsive Wettability for Efficient Oil-Water Separation. *Carbohydr. Polym.* **2020**, *237*, https://doi.org/10.1016/j.carbpol.2020.116133.
3. Yuba, E. Development of Functional Liposomes by Modification of Stimuli-Responsive Materials and Their Biomedical Applications. *J. Mater. Chem. B* **2020**, *8*, 1093–1107, https://doi.org/10.1039/c9tb02470k.
4. Vidallon, M.L.P.; Douek, A.M.; Quek, A.; McLiesh, H.; Kaslin, J.; Tabor, R.F.; Bishop, A.I.; Teo, B.M. Gas-Generating, PH-Responsive Calcium Carbonate Hybrid Particles with Biomimetic Coating for Contrast-Enhanced Ultrasound Imaging. *Part. Part. Syst. Charact.* **2020**, *37*, 1–8, https://doi.org/10.1002/ppsc.201900471.
5. Palanikumar, L.; Al-Hosani, S.; Kalmouni, M.; Nguyen, V.P.; Ali, L.; Pasricha, R.; Barrera, F.N.; Magzoub, M. pH-Responsive High Stability Polymeric Nanoparticles for Targeted Delivery of Anticancer Therapeutics. *Commun. Biol.* **2020**, *3*, 1–17, https://doi.org/10.1038/s42003-020-0817-4.
6. Ko, Y.; Jeong, H. Y.; Kwon, G.; Kim, D.; Lee, C.; You, J. PH-Responsive Polyaniline/Polyethylene Glycol Composite Arrays for Colorimetric Sensor Application. *Sensors Actuators, B Chem.* **2020**, *305*, https://doi.org/10.1016/j.snb.2019.127447.
7. Brighenti, R.; Li, Y.; Vernerey, F.J. Smart Polymers for Advanced Applications: A Mechanical Perspective Review. *Front. Mater.* **2020**, *7*, 1–18, https://doi.org/10.3389/fmats.2020.00196.
8. Bratek-Skicki, A. Towards a New Class of Stimuli-Responsive Polymer-Based Materials – Recent Advances and Challenges. *Appl. Surf. Sci. Adv.* **2021**, *4*, https://doi.org/10.1016/j.apsadv.2021.100068.
9. Bhat, A.; Amanor-Boadu, J.M.; Guiseppi-Elie, A. Toward Impedimetric Measurement of Acidosis with a PH-Responsive Hydrogel Sensor. *ACS Sensors* **2020**, *5*, 500–509, https://doi.org/10.1021/acssensors.9b02336.
10. Fan, X.X.; Xie, R.; Zhao, Q.; Li, X.Y.; Ju, X.J.; Wang, W.; Liu, Z.; Chu, L.Y. Dual PH-Responsive Smart Gating Membranes. *J. Memb. Sci.* **2018**, *555*, 20–29, https://doi.org/10.1016/j.memsci.2018.03.028.
11. Stuart, M.A.C.; Huck, W.T.S.; Genzer, J.; Müller, M.; Ober, C.; Stamm, M.; Sukhorukov, G.B.; Szleifer, I.; Tsukruk, V.V.; Urban, M.; Winnik, F.; Zauscher, S.; Luzinov, I.; Minko, S. Emerging Applications of Stimuli-Responsive Polymer Materials. *Nat. Mater.* **2010**, *9*, 101–113, https://doi.org/10.1038/nmat2614.
12. Davis, A.; Nasser, F.; Lead, J.R.; Shi, Z. Development and Application of a Ratiometric Nanosensor for Measuring PH inside the Gastrointestinal Tract of Zooplankton. *Environ. Sci. Nano* **2020**, *7*, 1652–1660, https://doi.org/10.1039/c9en01300h.
13. Hendi, A.; Hassan, M.U.; Elsherif, M.; Alqattan, B.; Park, S.; Yetisen, A.K.; Butt, H. Healthcare Applications of PH-Sensitive Hydrogel-Based Devices: A Review. *Int. J. Nanomedicine* **2020**, *15*, 3887–3901, https://doi.org/10.2147/IJN.S245743.
14. Broesder, A.; Woerdenbag, H.J.; Prins, G.H.; Nguyen, D.N.; Frijlink, H.W.; Hinrichs, W.L.J. PH-Dependent Ileocolonic Drug Delivery, Part I: In Vitro and Clinical Evaluation of Novel Systems. *Drug Discov. Today* **2020**, *25*, 1362–1373, https://doi.org/10.1016/j.drudis.2020.06.011.
15. Liu, Z.; Wang, W.; Xie, R.; Ju, X. J.; Chu, L. Y. Stimuli-Responsive Smart Gating Membranes. *Chem. Soc. Rev.* **2016**, *45* (3), 460–475. https://doi.org/10.1039/c5cs00692a.
16. Chu, L.-Y. *Smart Membrane Materials and Systems*. **2011**; https://doi.org/10.1007/978-3-642-18114-6.
17. Chu, L.-Y.; Li, Y.; Zhu, J.-H.; Wang, H.-D.; Liang, Y.-J. Control of pore size and permeability of a glucose-responsive gating membrane for insulin delivery. *Journal of Controlled Release* **2004**, *97*, 43-53, https://doi.org/10.1016/j.jconrel.2004.02.026.
18. Qu, J.B.; Chu, L.Y.; Yang, M.; Xie, R.; Hu, L.; Chen, W.M. A pH-Responsive Gating Membrane System with Pumping Effects for Improved Controlled Release. *Advanced Functional Materials* **2006**, *16*, 1865-1872, https://doi.org/10.1002/adfm.200500897.
19. Hou, X. Smart Gating Membranes: Smart Gating Multi-Scale Pore/Channel-Based Membranes (Adv. Mater. 33/2016). *Advanced Materials* **2016**, *28*, 7048-7048, https://doi.org/10.1002/adma.201670231.
20. Chu, L.; Xie, R.; Ju, X. Stimuli-responsive Membranes: Smart Tools for Controllable Mass-transfer and Separation Processes. *Chinese Journal of Chemical Engineering* **2011**, *19*, 891-903, https://doi.org/10.1016/S1004-9541(11)60070-0.
21. Gupta, R.; Ghosh, A.; Singh, A.K.; Misra, A. Clinical considerations for patients with diabetes in times of COVID-19 epidemic. *Diabetes & metabolic syndrome* **2020**, *14*, 211-212, https://doi.org/10.1016/j.dsx.2020.03.002.
22. Guo, W.; Li, M.; Dong, Y.; Zhou, H.; Zhang, Z.; Tian, C.; Qin, R.; Wang, H.; Shen, Y.; Du, K.; Zhao, L.; Fan, H.; Luo, S.; Hu, D. Diabetes is a risk factor for the progression and prognosis of COVID-19. *Diabetes/Metabolism Research and Reviews* **2020**, *36*, 1–9, https://doi.org/10.1002/dmrr.3319.
23. Erener, S. Diabetes, infection risk and COVID-19. *Molecular Metabolism* **2020**, *39*, https://doi.org/10.1016/j.molmet.2020.101044.
24. Rai, V.K.; Mishra, N.; Agrawal, A.K.; Jain, S.; Yadav, N.P. Novel drug delivery system: an immense hope for diabetics. *Drug Delivery* **2016**, *23*, 2371-2390, https://doi.org/10.3109/10717544.2014.991001.
25. Zhang, K.; Wu, X.Y. Modulated insulin permeation across a glucose-sensitive polymeric composite membrane. *Journal of Controlled Release* **2002**, *80*, 169-178, https://doi.org/10.1016/S0168-3659(02)00024-X.

26. Imanishi, Y.; Ito, Y. Glucose-sensitive insulin-releasing molecular systems. *Pure and applied chemistry* **1995**, *67*, 2015-2021.
27. Galaev, I.Y.; Mattiasson, B. 'Smart' polymers and what they could do in biotechnology and medicine. *Trends in Biotechnology* **1999**, *17*, 335-340, https://doi.org/10.1016/S0167-7799(99)01345-1.
28. Patil, R.S.; Sancaktar, E. Fabrication of PH-Responsive Polyimide Polyacrylic Acid Smart Gating Membranes: Ultrafast Method Using 248 Nm Krypton Fluoride Excimer Laser. *ACS Appl. Mater. Interfaces* **2021**, *13*, 24431–24441, https://doi.org/10.1021/acsami.1c01265.
29. Patil, R.S.; Sancaktar, E. Effect of solution parameters on pH-response of polyacrylic acid grafted polyimide smart membrane fabricated using 248 nm krypton fluoride excimer laser. *Polymer* **2021**, *233*, https://doi.org/10.1016/j.polymer.2021.124181.
30. Tiwari, A.; Sancaktar, E. Poly (N-isopropylacrylamide) grafted temperature responsive PET membranes: An ultrafast method for membrane processing using KrF excimer laser at 248 nm. *Journal of Membrane Science* **2018**, *552*, 357-366, https://doi.org/10.1016/j.memsci.2018.02.017.
31. Tiwari, A.; Sancaktar, E. Poly(N-isopropylacrylamide) grafting solution parameters for controlling temperature responsiveness in PET membranes fabricated using 248 nm KrF excimer laser. *European Polymer Journal* **2018**, *103*, 220-227, https://doi.org/10.1016/j.eurpolymj.2018.04.014.
32. Wu, L.; Sancaktar, E. Effect of PET support membrane thickness on water permeation behavior of thermally responsive PNIPAM-g-PET membranes. *Journal of Membrane Science* **2020**, *610*, https://doi.org/10.1016/j.memsci.2020.118304.
33. Sun, Y.; Lacour, S.P.; Brooks, R.A.; Rushton, N.; Fawcett, J.; Cameron, R.E. Assessment of the biocompatibility of photosensitive polyimide for implantable medical device use. *Journal of Biomedical Materials Research Part A* **2009**, *90A*, 648-655, https://doi.org/10.1002/jbm.a.32125.
34. Shiraishi, Y.; Miyamoto, R.; Zhang, X.; Hirai, T. Rhodamine-Based Fluorescent Thermometer Exhibiting Selective Emission Enhancement at a Specific Temperature Range. *Organic Letters* **2007**, *9*, 3921-3924, https://doi.org/10.1021/ol701542m.
35. Kono, K.; Imanishi, Y. An Insulin Release System That Is Responsive to Glucose. *J. Control. Release* **1989**, *10*, 195–203.
36. Thomas, J.; Singh, V.; Jain, R. Synthesis and characterization of solvent free acrylic copolymer for polyurethane coatings. *Progress in Organic Coatings* **2020**, *145*, https://doi.org/10.1016/j.porgcoat.2020.105677.
37. Shiraishi, Y.; Miyamoto, R.; Xuan, Z.; Hirai, T. Rhodamine-Based Fluorescent Thermometer Exhibiting Selective Emission Enhancement at a Specific Temperature Range. Org. Lett. 2007, 9, 3921–3924, https://doi.org/10.1021/ol701542m .

Supplementary Data

NH_2-Rhodamine B dye was synthesized following a reported procedure.[37] Rhodamine B (0.6g, 1.3mmol) and hexamethylenediamine (1.6g, 13.8 mmol) were dissolved in ethanol (50 mL). After refluxing for 18 h, the solvent was removed under vacuum. The crude was dissolved in an aqueous HCl solution (1M, 50mL). 1M of NaOH solution was added slowly to the acidic crude solution until a pink precipitate could be observed. The product was collected by filtration and washed excessively with DI water, and dried in a vacuum oven at 50°C overnight to yield a pink solid product (0.6g, 0.74mmol, 57% yield).

^{1}H-NMR (300 MHz, cdcl$_3$) δ 7.88 (t, 1H), 7.42 (t, 2H), 7.06 (d, 1H), 6.24 - 6.44 (m, 6H), 3.34 (q, 8H), 3.09 (t, 2H), 2.56 (t, 2H), 1.25 - 1.08 (m, 20H).

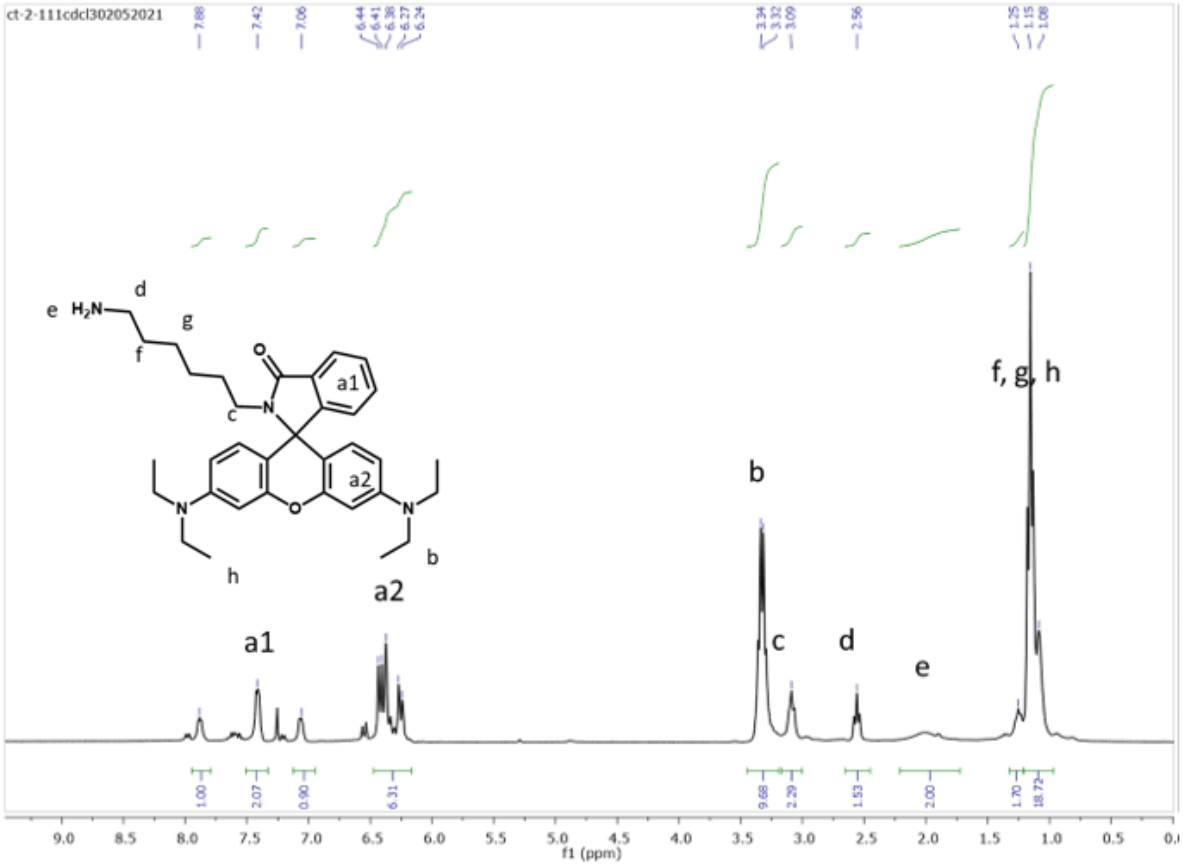

Figure S1. NMR spectra of NH_2-Rhodamine B.